7th International Symposium on Materials for Energy Storage and Conversion

&

11th International Conference on Nanomaterials and Advanced Energy Storage System

Book of Abstracts/Proceedings

17-21 July 2023
Muğla Sıtkı Koçman University

book of abstracts/proceedings
ISBN 978-625-00-8198-3

mesc-is.org
iness.kz

mESC-IS 2023

The Seventh International Symposium on Materials for Energy Storage and Conversion

INESS 2023

The Eleventh International Conference on Nanomaterials and Advanced Energy Storage System

Edited by
Ezgi Onur Şahin

17-21 July 2023
Mugla Sıtkı Koçman University

ISBN 978-625-00-8198-3

Performance of a Homemade Vanadium-Manganese Redox Flow Battery using Electrospun Carbon Electrode Catalyst and its Preliminary System Integration

Barun Kumar Chakrabarti [1,2,*], Mengzheng Ouyang [2], Metin Gencten [3], Zhiming Yan [4], Yashar S. Hajimolana [5*], Abhishek K. Singh [5], J. Rubio-Garcia [6], Abu Yousuf [7], Pejman Kazempoor [7], Chee Tong John Low [8], Yucel Sahin [9], and Nigel P. Brandon [2,10]

[1] Sabanci University Nanotechnology Research and Application Center, Tuzla, Istanbul 34956, Turkey
[2] Department of Earth Science and Engineering, Imperial College London, South Kensington, London SW7 2AZ, UK
[3] Yildiz Technical University, Faculty of Chemical and Metallurgical Engineering, Department of Metallurgy and Materials Engineering, 34210 Istanbul, Turkey
[4] Battery Recycling Lab, WMG, University of Warwick, Coventry CV4 7AL, UK
[5] Department of Thermal and Fluid Engineering, University of Twente, 7500 AE, Enschede, The Netherlands
[6] Department of Chemistry, Faculty of Science, Imperial College London, South Kensington, London SW7 2AZ, UK
[7] Aerospace and Mechanical Engineering, University of Oklahoma, OK, USA
[8] WMG, Warwick Electrochemical Engineering Group, Energy Innovation Centre, WMG, University of Warwick, Coventry CV4 7AL, UK
[9] Yildiz Technical University, Faculty of Art and Sciences, Department of Chemistry, 34220, Istanbul, Turkey
[10] RFC Power Ltd., London SW7 2PG, United Kingdom

Abstract

In this study, the possibility of enhancing the performance of the all vanadium redox flow battery (VRFB) and a vanadium/manganese redox flow battery (V/Mn RFB) using carbonized catalyst layers (CCLs) prepared via electrospinning is considered. To display performance enhancement caused by such catalysts, a home made reactor with non optimized compression and serpentine flow fields was employed. This reactor was manufact-ured using a combinati-on of recycled metals, graphite and chemically resistant plastic, with serpentine flow fields engraved using in house computer aided manufacture employing SolidWorks software. The surface morphologies of the graphite and car-bon based electrodes used during electrochemical tests were characterized by SEM and XRD analyses. For such a non opt-imized reactor, the application of the CCL as an additional material to an as received graphite felt electrode show-s improvements for both vanadium based RFB technologies. For instance, the en-hancements in power densities of VRFBs were achieved by 30% improv-ement in peak power density using CCL. V/Mn flow batteries showed 50% improvement in capacity utilization when using CCL. It is also postulated that because the CCL needs to be placed between the flow fields and the felt electrodes to prevent fiber protrusion into the flow channels when compressed in the reactor, the peak power densities and cycling efficiencies were lower than those reported for optimized RFBs in the literature. The need to improve the power density is a critical consideration for RFBs. A high power density translates into lower capital costs for V/Mn RFBs, which translates into an effective system integrat-ion for grid scale load levelling, water desalination or renewable energy storage.

1.Introduction

The vanadium/manganese (V/Mn) redox flow battery can achieve a higher energy density of 35 W h L ^{1} than all vanadium redox flow batteries (VRFBs), owing to its higher cell voltage (1.77 V) [1]. The V/Mn syst¯em utilizes- V(II)/V(III) redox couples as the negative electrolyte and Mn(II)/Mn(III) redox couples as the positive electrolyte [2].

In spite of the high energy density for the V/Mn RFB, it faces drawbacks owing to Mn^{3+} instability that, in turn, results in precipitation of manganese dioxide thereby causing severe capacity fade [3]. To diminish this problem, a few investigations reported on the use of TiO^{2+} to stabilize the electrolytes [3 5]. Besides the mitigation of manganese dioxide precipitates, both VRFBs and V/Mn RFBs have displayed per¯fo rmance drops due to insufficient electrode wetting of the graphite felt electrodes, thereby suffering from high mass transport polarizations [6]. Thermally or chemically treating the felts provide some performance enhancement [7]

Barun Chakrabarti

Dr Barun K. Chakrabarti has recently joined SUNUM since March 2023. His last role was as a Postdoctoral Research Fellow in WMG at the University of Warwick. He completed his MEng in Chemical Engineering at Imperial College London and a PhD on Regenerative Fuel Cells at the University of Manchester, UK. He has studied a wide range of electrochemical technologies for energy and environmental applications. His current research focuses on hydrogen-based redox flow batteries, electrospinning, electrochemical regeneration of lithium-ion battery cathodic materials, and electrophoretic deposition of nanomaterials including graphene. He has over 60 journal publications including Nature Communications.

Corresponding author: Barun Chakrabarti, e-mail: barun.chakrabarti@sabanciuniv.edu, tel: 021-6568-7942

but a more economically robust means for solving such issues could involve the application of other electrode catalysts involving carbonized nanosheets, graphene or carbon nanotubes [7, 8]. Electrospinning has been employed as an effective means to prepare carbonized fibrous mats [7] to provide enhanced performances in VRFBs [9] and of late in a hydrogen/vanadium hybrid flow battery [10]. However, the application of such nanomaterial electrode catalysts or stand-alone electrodes prepared by means of electrospinning has not been studied significantly for other redox couples and their evaluation for V/Mn RFBs could be a step forward towards investigations with other RFB electrolytes.

In this work, carbonized catalyst layers (CCLs manufactured in-house by means of electrospinning and carbonization) were evaluated in both VRFB and V/Mn RFB systems. The graphite felt control electrode was deliberately not activated thermally or chemically to understand the effect of CCLs in both RFBs. The RFB used herein was homemade in order to consider potential issues that could arise from non-optimised flow field design, electrode compression and other factors. The main reason for using a non-optimized reactor (unlike Scribner ones employed in our previous studies [11]) is to try and highlight the performance enhancements that could be achieved solely by using CCLs and at reduced capital investments. However, low power densities were determined, which result in high costs, due to which more studies are required to improve the electrochemical features of CCL. If that can be successfully achieved, then V/Mn RFBs may be integrated with renewable energies resulting in lower carbon footprints of electricity generation. A brief consideration of this has also been reported herein to emphasize the importance of V/Mn RFBs due to their flexible energy to power ratio as well as a decent control complexity in comparison to other battery technologies (owing to the employment of active elements such as pumps for electrolyte flow) when applied for systems integration for grid-scale electricity generation, storage and supply.

2. Experimental

2.1. Chemicals and Electrolytes

Iron acetylacetonate [$Fe(acac)_3$] was obtained from Sigma-Aldrich (≥97%, Dorset, UK), N,N'-dimethylformamide (DMF, Technical grade for electrospinning, ~94% pure) was purchased from VWR International (Leicestershire, UK) and polyacrylonitrile (PAN) was sourced from Goodfellow Cambridge Limited Huntingdon (average particle size ~50 µm, molecular weight ~230,000 g mol^{-1}). Vanadium (IV) oxide sulfate (hydrated) was purchased from Sigma-Aldrich (purity > 99%, Dorset, UK). $MnCO_3$ (Sigma-Aldrich, ≥99.9% trace metal basis from Dorset, UK) was used as received. $TiOSO_4$ (Sigma-Aldrich from Dorset, UK) was added to the manganese electrolyte solution only to prevent the precipitation of MnO_2 as discussed elsewhere [12]. This Mn-Ti electrolyte was used for the V/Mn RFB system. Sulfuric acid (5 M) was obtained from Fluka (Dorset, UK). All chemicals were used without further purifications. All solutions were prepared by using deionized water (18 MΩ) and all chemicals were of analytical grade, where not specified.

2.2. Membrane-Electrode-Assembly (MEA)

A well hydrated Nafion 115 membrane (127 µm thick, Fuel Cell Store, Texas, USA) was sandwiched between both electrodes (anode and cathode) to prepare the membrane-electrode-assembly (MEA). The membrane was pre-treated in 1 M H_2SO_4 solution for 1 h at 80 °C and then rinsed with de-ionized water. Graphite felts (4.6 mm thick, SGL group, Germany, Sigracell GFD4,6 EA) and CCLs (100 µm thick - homemade) were not pre-treated and used as received for VRFB and V/Mn systems. CCL was made via a combination of electrospinning and carbonization as detailed elsewhere [11].

2.3. Morphological Analysis

The surface morphologies of the graphite and carbon-based electrodes used during electrochemical tests were characterized by SEM analysis. This was performed using a Zeiss Sigma FEG-SEM instrument. XRD was performed using an Aeris desktop machine with data analysis performed by means of Highscore software (Malvern Panalytical).

2.4. Redox Flow Battery Cell Assembly

Battery testing was conducted using a 5 cm^2 single cell (designed in-house). The fabricated VRFB hardware consisted of two aluminium endplates (sourced from workshop waste), copper current collectors (also from workshop waste), and graphite plate with serpentine flow fields (engraved in-house using a computer-aided manufacturing machine, operated via SolidWorks software). The positive and negative electrodes were separated by a Nafion 115 ion-exchange membrane. The electrodes were made of graphite felt at both the positive and negative sides of the cell for investigating classical RFB behaviour. The electrodes were modified by adding CCL on the flow channels with the felts facing the membrane for additional experiments to determine the influence of CCL upon RFB performance. Viton gaskets (J-Flex) were placed between the different parts of the cell to prevent leakage of the electrolyte, and to allow a reasonable compression of the electrode. The entire cell was compressed to 2 Nm torque to avoid carbon felt deformation, without obtruding the flow channels whilst avoiding leaks. This torque was much lower to those applied when assembling commercially sourced Scribner flow cells [11], which could have caused significant performance drops. Higher compressions could ensure better electrode performance but at the cost of blocking the flow channels with graphite fibers and/or CCL fracture (when using them with felt) that could increase pressure drops and mass transport polarizations.

2.5. Experimental Operation for VRFB and V/Mn RFB

All experiments were carried out at 20 °C. The all-vanadium electrolyte was initially made by dissolution of 1 M $VOSO_4$ (99.9% purity, Alfa Aesar) in a sulfuric acid solution of 5 M concentration [12]. Both electrolyte reservoirs initially consisted of a solution of vanadium (IV) ions. The positive electrolyte volume was initially twice the negative electrolyte volume to account for the double electron transfer reaction that is needed on the negative side to convert vanadium (IV) into vanadium (II) ions. These electrolytes were then charged until the vanadium (IV) was fully converted to vanadium (II) and vanadium (V) for the negative and positive electrolytes, respectively. Half of the electrolyte on the positive side was then removed from its reservoir, making the volumes on each

side identical for consequent experiments [13]. The negative and positive electrolyte tanks are filled with the prepared electrolyte to a volume of 100 ml and pumped (Cole Parmer Masterflex Model 77200-50) to the negative and positive half cells, respectively. The negative reservoirs were purged with N_2 gas (BOC) and sealed before the single-cell test to prevent oxidation of V(II) in air or via dissolved oxygen.

The galvanostatic tests were performed using a Bio-Logic potentiostat (VSP-300) with a 10 A booster and data logging was performed using EC-Lab software. For all tests, the system was allowed to reach an upper cut-off voltage of 1.8 V and a lower cut-off voltage of 0.8 V for VRFBs. These values were changed to 2.1 V (upper cut-off) and 0.6 V (lower cut-off) when evaluating the V/Mn RFB. This was done to ensure high electrolyte utilization and to try and minimize side reactions such as hydrogen evolution. Several-cycle charge-discharge tests were performed at constant current densities in the range of 20−100 mA cm^{-2} for the VRFB and V/Mn RFB.

Finally, potential-current density curves were obtained at an initial state-of-charge (SoC) of 100%, by applying steps of galvanostatic discharge at constant current densities in the range of 40−500 mA cm^{-2} (30 s discharge followed by 120 s rest between each discharge step). Cycling was carried out between 50 and 100 mA cm^{-2}. Electrolyte utilization was determined at 80 mA cm^{-2}. Efficiencies were also determined at 80 mA cm^{-2}.

3. Results and Discussion

3.1. VRFB performance using Electrospun CCL and graphite felt electrodes

The power densities of the VRFB using graphite felts and compared with the same system employing CCLs is shown in Fig. 1. The CCL appears to improve the peak power density (almost 250 mW cm^{-2}) by approximately 30% compared to just using the untreated graphite felt (slightly in excess of 210 mW cm^{-2}). A similar performance advantage is also noticed for electrolyte capacity when using the CCL in combination with felt electrodes (Figure 1b, which shows that the cell capacity utilization when using felt electrodes only was less than 200 mA h but this increased to almost 250 mA h when CCL was used along with felt electrodes).

(a)

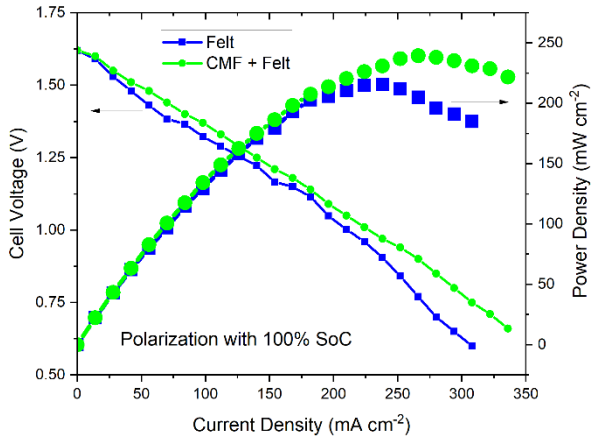

(b)

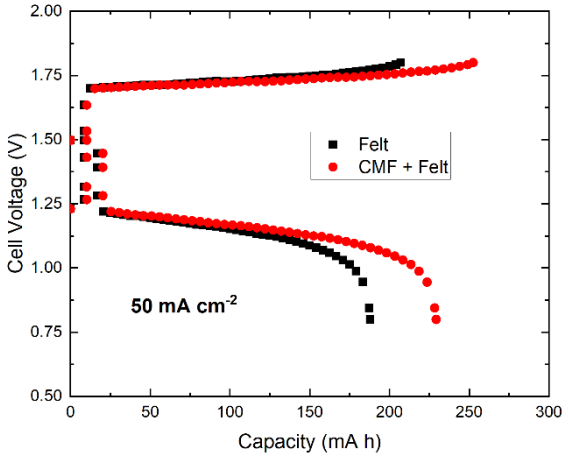

Fig. 1. Polarization and power density curves for VRFB. System condition = 1 M $VOSO_4$ in 5 M H_2SO_4 (initial electrolyte composition), 50 ml min^{-1} flow, 100 ml volume (each), less than 20% electrode compression, room temperature and negative half-cell was maintained with an inert nitrogen blanket to prevent V^{2+} spontaneous oxidation to V^{3+} (which occurs in the presence of oxygen). CCL was placed in between the graphite felt and the flow channels in both half-cells.

The better wetting of electrodes due to the presence of carbon nanotubes (CNTs, present in the hair-like structures of CCLs) may also be deciphered from qualitative morphological analyses as discussed as follows. Fig. 2 shows the XRD patterns for graphite felt samples compared with those of CCL. The peaks associated for graphite felt is identical to that reported in the literature [14]. Also, peaks depicting presence of iron and carbon are prominent for CCL. Additionally, CCL appears to have more disorder than felt due to the presence of hair-like CNTs, which could have contributed to the improved catalytic performance of the material as reported recently for a hydrogen/vanadium hybrid flow battery [11]. Additionally, the SEM images of both carbon materials are provided as insets with their respective XRD images in Fig. 2. CCL has more bundles of fibers along with “hair-like” outgrowths that may improve access of electrolyte to active electrode areas for the vanadium ions to undergo fast charge transfer in comparison to the untreated graphite felt. It seems evident, also from previous studies [14], that CCL is able to catalyze liquid-based redox reactions more effectively when combined with a commercial electrode such as carbon cloth or graphite felt.

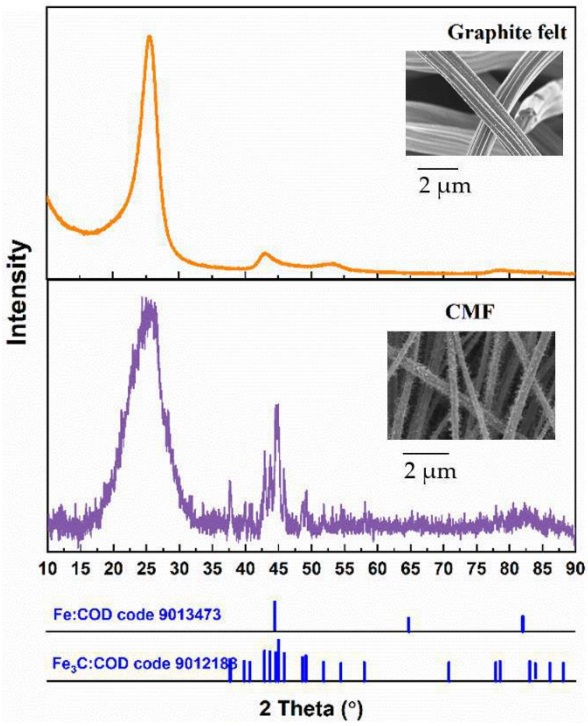

Fig. 2. XRD image of graphite felt compared with that of CCL (respective SEM images are given in the inset). SEM image of CCL (referred to as CMF in the figure) shows typical hair-like structures that contain CNTs.

3.2. V/Mn Flow Battery

1 M vanadium sulphate in 5 M sulfuric acid was used as the catholyte while 1 M manganese carbonate was dissolved in 5 M sulfuric acid with 1 M titanium sulphate as the anolyte. The titanium salt is used to prevent an irreversible conversion of manganese ions to manganese dioxide precipitates that usually lower electrolyte capacity. Fig. 3(a) shows the power density curves for the V/Mn flow battery. The presence of CCL resulted in a 35% enhancement of the peak power density (for V/Mn RFB using only graphite felt electrodes the power density was just under 40 mW cm^{-2} while the counterpart using CCL along with felts gave a higher peak power density of about 60 mW cm^{-2}), which is a good comparative result. Electrolyte capacity also appears to show about 50% improvement when using CCLs (Fig. 3b). The observation of two voltage discharge plateaus is most due to likely vanadium crossover to the manganese half-cell. First plateau could be related with Mn(III) conversion to Mn(II) while the second plateau could be associated with V(V) reduction to V(IV). It is most likely that the presence of V and Ti ions simultaneously contribute to inhibit MnO_2 precipitate formation, thereby mitigating capacity fading.

The results shown in Fig. 3 indicate that CCL works very well as an electrode catalyst for both vanadium and manganese RFBs. Despite that, the KPI values are still very low when compared with the literature [15, 16] and this is because of the use of a non-optimized reactor that involved placing the CCL between the flow channels and the felt electrodes to prevent fluid flow blockages due to protruding graphite fibers. This, in addition to low compression of the electrodes also may have reduced the electrochemical surface area for electron transfer reactions to occur. If a commercially sourced Scribner flow cell was employed then the CCL could be successfully placed in between the felt and the membrane, which could enhance performances significantly as discussed in the subsequent section.

(a)

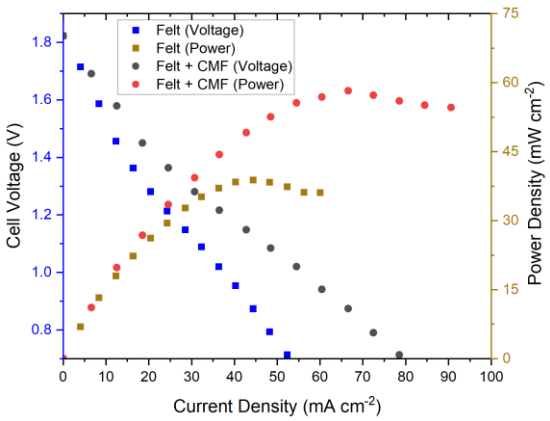

(b)

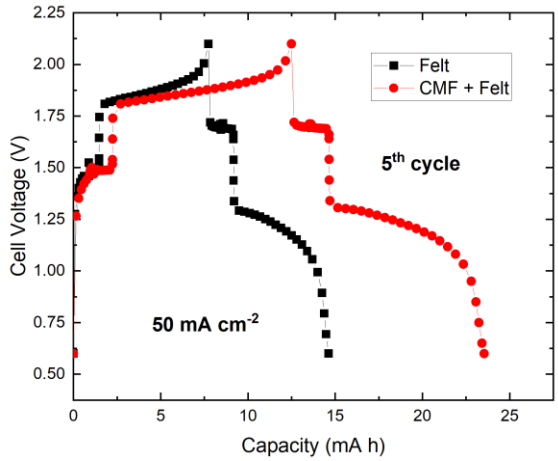

Fig. 3. (a) Polarization and power density curves for V/Mn RFB. (b) Cell capacity graph. System condition = 1 M $VOSO_4$ in 5 M H_2SO_4 for initial catholyte and 1 M $MnCO_3$ in 5 M H_2SO_4 with 1 M $TiOSO_4$ for initial anolyte, 50 ml min^{-1} flow, 100 ml volume (each), < 20% electrode compression (non-optimized), room temperature operation. CCL was placed in between the graphite felt and the flow channels in both half-cells.

3.3. System Integration of V/Mn Flow Battery

The purpose of this section is to consider the value of a vanadium/manganese redox flow battery (V/Mn RFB) as a potential commercially viable replacement for VRFBs owing to its lower costs associated with replacing vanadium electrolytes with more ubiquitous and therefore economical manganese-based electrolytes. This section therefore provides a brief qualitative consideration on how an optimized V/Mn RFB can be integrated effectively with the electric grid,

renewable energy supply and/or water desalination plants. In this regard, Fig. 4 shows how the V/Mn RFB can be integrated with a solar PV or with wind turbines to provide support for a combined heat and gas powered (CHP) supply system. By means of a reversible solid oxide (RSO) cell, hydrogen, carbon monoxide and methane can be generated from excess renewable energy. Methanation reaction can also be performed inside the stack. However, 100% conversion cannot be achieved. The hydrogen may be stored or supplied directly to gas grids as shown in Fig. 4. In this manner, load levelling may be effectively achieved.

The RSO cell utilizes steam and carbon dioxide input streams that are generated from the CHP plant. The RSO cell produces carbon monoxide that can be applied as an input stream for a methanation unit, which can convert CO to methane or methanol. The latter can be implemented as a fuel or in fuel cells while the methane gas may be recycled to the CHP plant. The CHP may also be implemented for effective load balancing. The CHP system can use oxygen sweep gas generated by the RSO cell to optimize the combustion process and reduce other emissions. In this regard, the CHP is best employed for baseload power output rather than for peak load energy or electricity supply.

The CO_2 from the CHP exhaust gases may be captured and fed to the RSO cell, thus establishing the circularity of the carbon in the proposed configuration (Fig. 4). The H_2 can be input to the methanation process for hydrogenation of carbon monoxide (CO) to methane/methanol. Similarly, the thermal energy from the CHP may be employed for steam generation which could be used for H_2 production by the RSO cell. The V/Mn RFB can also act as a potential energy storage for a water desalination process. A typical water desalination plant needs energy intensive operation for high-pressure pumping of the saline water to the separation membrane assembly. Due to the significant amount of water to be pumped, this component requires considerable electricity input which could be supplied by renewable energy sources, like solar and wind.

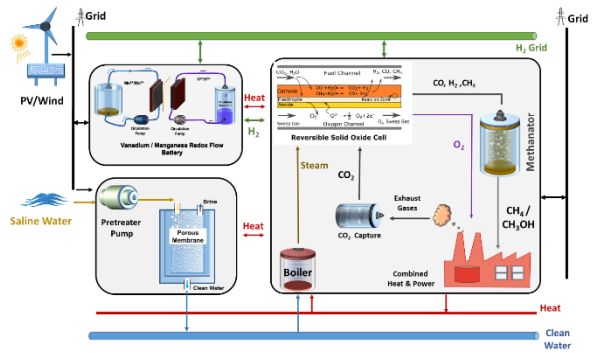

Fig. 4. Schematic depicting the proposed integration of the V/Mn RFB in a renewable energy powered integrated system for power, heat and gas generation and water desalination system. Adapted from a similar study reported by ACS on hydrogen/vanadium regenerative fuel cells [11].

Additionally, the excess electricity from renewable sources can be utilized by the RSO cell for H_2 generation, which may be stored for power generation when the renewable electricity is not available, thus facilitating continuous generation of electricity for the water desalination process.

4. Conclusion

This study shows the application of carbonized catalyst layers (homemade using electrospinning and carbonization) for improving performances for both VRFBs and V/Mn RFBs. The reactor used for these tests were also homemade, with limitations in non-optimized compression, fluid dynamics and other factors. Key performance indicators (KPIs) investigated in this work were limited to polarization curves and charge/discharge cycling efficiencies. The use of untreated graphite felts as control electrodes resulted in poor performances of both VRFB and V/Mn RFB systems but this was done deliberately to ascertain the effect of CCLs on KPIs. It was noted for VRFBs that peak power densities were about 40% higher when using CCLs, but energy efficiencies were not significantly improved (by approximately 15%) upon cycling. This is most likely because the CCL had to be placed in between the flow channels and felt electrodes to prevent graphite fibers from protruding into the flow fields and disturbing/blocking the fluid dynamics of the electrolytes. It is also hypothesized that the CCLs being brittle could have broken off during the cycling, possibly due to high initial overpotentials and uneven pressure exerted by the non-optimized reactor that could have broken some of the CCLs. Considering these results, the V/Mn RFB was not cycled much and the KPIs noted for peak power densities (35% improvement when using CCL in combination with graphite felt), and capacity utilization (50% higher when using CCL with graphite felt electrodes) suggest that further investigations with more robust versions of the CCLs could yield more optimized outputs, which could be considered for other redox couples for homemade and yet economical RFB reactors. Better KPIs leading to enhanced capacities and power outputs for V/Mn RFBs can lead to pilot scale testing by combining with renewable energy storage or water desalination plants for effective system integration investigations as further work.

Acknowledgement

This research was partly funded by the EPSRC project Lower Cost and Longer Life Flow Batteries for Grid Scale Energy Storage (EP/L014289/1) and partly by EPSRC ISCF Wave 1: 3D electrodes from 2D materials (EP/R023034/1).

References

[1] Reynard, D., et al., Chemistry – A European Journal 26 (2020) 7250-7257.
[2] He, Z., et al., Journal of Renewable and Sustainable Energy 6 (2014) 053124.
[3] Rubio-Garcia, J., et al. Journal of Physics: Energy 1 (2019) 015006.
[4] Reynard, D. and Girault, H. Cell Reports Physical Science 2 (2021) 100556.
[5] Tokuda, K., et al., The Journal of Chemical Physics 149 (2018) 014503.
[6] Chakrabarti, B. K., et al. Sustainable Energy & Fuels 4 (2020) 5433-5468.
[7] Flox, C., et al., RSC Advances 3 (2013) 12056-12059.
[8] Chakrabarti, B., et al., ChemElectroChem 4 (2017) 194-200.
[9] Iskandarani, B. et al., Energy & Fuels 36 (2022) 9282-9294.

[10] Sun, J., et al., Journal of Power Sources 470 (2020) 228441.
[11] Chakrabarti, B. K., et al. ACS Applied Nano Materials 4 (2021) 10754-10763.
[12] Chakrabarti, B. K., et al. ACS Applied Materials & Interfaces 12 (2020) 53869–53878.
[13] Chakrabarti, B., et al. International Journal of Hydrogen Energy 44 (2019) 30093-30107.
[14] Zhang, L., et al., RSC Advances 10 (2020) 13374-13378.
[15] Zhang, L., et al., Journal of Power Sources 242 (2013) 15-22.
[16] Ersozoglu, M. G., et al., International Journal of Energy Research 45 (2021) 2126-2137.
[17] Lee, H. J., Park, S., and Kim, H., Journal of The Electrochemical Society 165 (2018) A952-A956.